Light-Controlled Directional Liquid Drop Movement on TiO$_2$ Nanorods-Based Nanocomposite Photopatterns

Francesca Villafiorita Monteleone,*[,†,§] Gianvito Caputo,[†] Claudio Canale,[‡] P. Davide Cozzoli,[†] Roberto Cingolani,[‡] Despina Fragouli,[§] and Athanassia Athanassiou*[,†,§]

[†]National Nanotechnology Laboratory (NNL), CNR - Istituto di Nanoscienze, Università del Salento, via per Arnesano, 73100 Lecce, Italy, [‡]Italian Institute of Technology (IIT), via Morego 30, 16152 Genova, Italy, and [§]Center for Biomolecular Nanotechnologies (CBN) of IIT @UniLe, via Barsanti, 73010 Arnesano, Lecce, Italy

Patterned polymeric coatings enriched with colloidal TiO$_2$ nanorods and prepared by photopolymerization are found to exhibit a remarkable increase in their water wettability when irradiated with UV laser light. The effect can be completely reversed using successive storage in vacuum and dark ambient environment. By exploiting the enhancement of the nanocomposites hydrophilicity upon UV irradiation, we prepare wettability gradients along the surfaces by irradiating adjacent surface areas with increasing time. The gradients are carefully designed to achieve directional movement of water drops along them, taking into account the hysteresis effect that opposes the movement as well as the change in the shape of the drop during its motion. The accomplishment of surface paths for liquid flow, along which the hydrophilicity gradually increases, opens the way to a vast number of potential applications in microfluidics.

Introduction

In recent years, the realization of microfluidic devices has attracted great interest thanks to the variety of their potential applications, such as in biochemical analysis and combinatorial chemical synthesis.[1−3] These systems are very useful for transporting, storing, mixing, reacting, and analyzing small amounts of diverse liquids. A major challenge in their operation is the controlled motion of liquids, achievable through capillary forces in the case of microstructures,[4] which are limited by the increased interfacial forces as the structures are miniaturized. A promising alternative method for liquid motion control that favors the manipulation of smaller liquid volumes is the spatially gradual change in the surfaces wettability, which can induce spontaneous movement of liquid drops from the hydrophobic to the hydrophilic areas of the surfaces. The use of smart materials that can respond to external stimuli by reversibly changing their surface properties has been employed several times[5−7] for the creation of flow paths along which the wettability is gradually increased. In such systems the surface properties can change reversibly by alternating an external stimulus, such as temperature, light, pH, voltage, and so on. Specifically, the use of light can facilitate the miniaturization of devices due to the absence of wires, cables, thermal components, containers, and so on. One of the most widely adopted solutions in the area of photoresponsive surfaces

for spontaneous liquid drop movement is the use of polymers that have side chains functionalized with photochromic molecules.[8−13] However, because the wettability variations achieved with these systems are inherently small (contact angle differences of ∼10° are typically measured),[8,10,12−17] it is quite complex to create sufficient wettability gradients to induce spontaneous movement of the liquid drops. In this respect, a more effective approach could be the use of semiconductor oxides, such as TiO$_2$, ZnO, WO$_3$, and V$_2$O$_5$, whose switchable wettability changes upon band gap photoexcitation are much more pronounced. The most prominent wettability differences have been achieved using different nanostructures, such as nanorods (NRs), nanotubes, or nanowires of TiO$_2$, ZnO, or WO$_x$ on surfaces, which can be switched from superhydrophobic to superhydrophilic upon UV irradiation.[18−21] Wang et al. demonstrated that this kind of surface can be used to move a drop from an easy sliding to a highly sticky, still superhydrophobic surface area by slightly tilting the substrate.[20] Kwak et al. also

*Corresponding authors. E-mail: francesca.villafiorita@unisalento.it (F.V.M.); athanassia.athanassiou@unisalento.it (A.A.).

(1) Halldorsson, J. A.; Little, S. J.; Diamond, D.; Spinks, G.; Wallace, G. *Langmuir* **2009**, *25*, 11137–11141.

(2) Feng, X.; Dua, W.; Luoa, Q.; Liu, B.-F. *Anal. Chim. Acta* **2009**, *650*, 83–97.

(3) Lee, S. J.; S., J.; Park, J. S.; Im, H. T; Jung, H., II. *Sens. Actuators, B* **2008**, *132*, 443–448.

(4) Juncker, D.; Schmid, H.; Drechsler, U.; Wolf, H.; Wolf, M.; Michel, B.; de Rooij, N.; Delamarche, E. *Anal. Chem.* **2002**, *74*, 6139–6144.

(5) Bain, C. D; Burnett·Hall, G. D.; Montgomerie, R. R. *Nature* **1994**, *372*, 414–415.

(6) Gallardo, B; Gupta, V. K.; Eagerton, F. D.; Jong, L. I; Craig, V. S.; Shah, R. R.; Abbott, N. L. *Science* **1999**, *283*, 57–60.

(7) Liang, L.; Feng, X.; Liu, J.; Rieke, P. C. *J. Appl. Polym. Sci.* **1999**, *72*, 1–11.

(8) Ichimura, K.; Oh, S.-K.; Nakagawa, M. *Science* **2000**, *288*, 1624–1626.

(9) Yang, D.; Piech, M.; Bell, N. S.; Gust, D.; Vail, S.; Garcia, A. A.; Schneider, J.; Park, C.-D.; Hayes, M. A.; Picraux, S. T. *Langmuir* **2007**, *23*, 10864–10872.

(10) Oh, S.-K.; Nakagawa, M.; Ichimura, K. *J. Mater. Chem.* **2002**, *12*, 2262–2269.

(11) Shin, J. Y.; Abbott, N. L. *Langmuir* **1999**, *15*, 4404–4410.

(12) Kausar, A.; Nagano, H.; Ogata, T.; Nonaka, T.; Kurihara, S. *Angew. Chem., Int. Ed.* **2009**, *48*, 2144–2147.

(13) Rosario, R.; Gust, D.; Garcia, A. A.; Hayes, M.; Taraci, J.; Clement, T.; Dailey, J. W.; Picraux, S. T. *J. Phys. Chem. B* **2004**, *108*, 12640–12642.

(14) Sandre, O.; Gorre-Talini, L.; Ajdari, A.; Prost, J; Silberzan, P. *Phys. Rev. E* **1999**, *60*, 2964–2972.

(15) Dos Santos, F. D.; Ondarçuhu, T. *Phys. Rev. Lett.* **1995**, *75*, 2972–2975.

(16) Athanassiou, A.; Lygeraki, M. I.; Pisignano, D.; Lakiotaki, K.; Varda, M.; Mele, E.; Fotakis, C.; Cingolani, R.; Anastasiadis, S. H. *Langmuir* **2006**, *22*, 2329–2333.

(17) Athanassiou, A.; Varda, M.; Mele, E.; Lygeraki, M. I.; Pisignano, D.; Farsari, M.; Fotakis, C.; Cingolati, R.; Anastasiadis, S. H. *Appl. Phys. A: Mater. Sci. Process.* **2006**, *83*, 351–356.

(18) Das, S. N.; Choi, J. H.; Kar, J. P.; Myoung, J. M. *Appl. Surf. Sci.* **2009**, *225*, 7319–7322.

(19) Feng, X.; Zhai, J.; Jiang, L. *Angew. Chem., Int. Ed.* **2005**, *44*, 5115–5118.

(20) Wang, D.; Liu, Y.; Liu, X.; Zhou, F.; Liua, W.; Xuea, Q. *Chem. Commun.* **2009**, 7018–7020.

(21) Kwak, G.; Lee, M.; Yong, K. *Langmuir* **2010**, *26*, 9964–9967.

presented the drop sliding on OTS-covered WO_x surfaces from a superhydrophobic to a superhydrophilic area, the latter created by UV irradiation. Also, in this case, the substrate needed to be tilted for the sliding to occur.[21] Here we present an alternative technique where a spontaneous and directional drop movement along defined paths of polymeric nanocomposite coatings is succeeded. The surfaces of polymeric nanocomposites can be the ideal candidates for spontaneous liquid drop movement because they combine the characteristics of the polymer matrices (e.g., processability, adhesion on substrates, optical clarity, solubility, low cost, etc.) with the large hydrophilicity increase attainable upon band gap photoexcitation of their inorganic nanofillers.

Specifically, we use colloidal titanium dioxide (TiO_2) NRs as nanofillers in photopolymerized poly(methyl methacrylate) (PMMA) matrix. The photopolymerization procedure offers the possibility of creating diverse nanocomposite patterns, and is accomplished by irradiating with UV light small amounts of solutions of methyl methacrylate (MMA) mixed with TiO_2 NRs, in the presence of a photoinitiator (PI), deposited on solid substrates. Next, the produced nanocomposites, subjected to UV light irradiation, exhibit fully controllable changes of their wettability characteristics by increasing the irradiation time. We prove that the increased hydrophilicity is due to the presence of TiO_2 NRs on the surface of the formed patterns. Indeed, upon UV irradiation of TiO_2, oxygen vacancies are created on the surface, resulting in the conversion of Ti^{4+} to Ti^{3+} sites. These sites are favorable for dissociative adsorption of atmospheric water molecules, in turn leading to the formation of a highly hydroxylated (hence, hydrophilic) surface. This procedure is reversible because upon long-term storage (a few months) under ambient dark conditions or for an accelerated process upon thermal treatment, vacuum storage, or visible irradiation,[21-26] the adsorbed hydroxyl groups can be removed and eventually replaced by ambient oxygen, allowing the initial hydrophobicity to be recovered.[22-24,28,29] Previous studies of our group proved that the irradiation conditions used in this work prevent the photocatalytic destruction of the pre-existing organic capping molecules of the TiO_2 surface.[26]

Finally, we take advantage of the controlled wettability changes to realize flow liquid paths. In particular, irradiating adjacent surface areas of specific dimensions with increasing time, we create wettability gradients along the surfaces, essential for liquid droplet motion. This is the very first time that the substantial, well-demonstrated, wettability properties of TiO_2 upon UV treatment are used for the creation of specific paths along nanocomposite surface coatings for droplet transport.

Experimental Section

Materials. All chemicals were used as received. MMA (99% purity) was purchased from Sigma-Aldrich. The PI IRGACURE1700 (25% bis(2,6-dimethoxy benzoyl) 2,4,4-trimethyl-pentyl-phosphineoxide, 75% 2-hydroxy-2-methyl-1-phenyl-propan-1-one

(DAROCURE1173)) was purchased from Ciba SpecialChem. The TiO_2 NRs solutions were prepared in toluene, as described by Cozzoli et al,[30] to obtain oleic-acid-capped TiO_2 NRs with a mean length of 20 nm and an average diameter of 3 nm. Glass microscope slides (Carlo Erba) were used as substrates. All solvents used were purchased from Carlo Erba.

Nanocomposites Preparation by Photopolymerization. Solutions of MMA, TiO_2 NRs, and PI in toluene were prepared at a concentration of 94, 5, and 1 wt %, respectively (Supporting Information, Figure S1). All solutions were stirred and left under dark for several minutes to equilibrate. Next, 200 μL of each solution was spin coated on glass substrates at 1000 rpm for 20 s to be subjected to photopolymerization. Finally, ~40 μL of the same solution was dropcasted onto each sample. To obtain the patterned PMMA/TiO_2 nanocomposite coatings, the previously spincoated and subsequently casted samples were irradiated with the third harmonic of a pulsed Nd:YAG laser (Quanta-Ray GCR-190, Spectra Physics) with an energy density of 10.5 mJ·cm^{-2} (λ = 355 nm, pulse duration = 4−6 ns, repetition rate = 10 Hz) for 90 min using aluminum photomasks with geometric features ranging from few micrometers to some centimeters. After the photopolymerization, each sample was washed three times with methanol to remove unreacted monomer and PI and then dried under ambient dark conditions for 2 days to achieve a complete solvent evaporation. Independent experiments have demonstrated that after the 2 day storage period the photopolymerized samples have stable apparent water contact angles (WCAs).

Photoirradiation and Storage Processes for Reversible Wettability Changes. To enhance the hydrophilicity of the TiO_2 NRs exposed on the surface of the photopolymerized nanocomposites, we irradiated the prepared films for 90 min with a pulsed Nd:YAG laser at 355 nm (energy density = 7 mJ·cm^{-2}, repetition rate = 10 Hz, pulse duration = 4−6 ns). We achieved the complete recovery of the initial wettability of the films by placing them in vacuum at a pressure of 3×10^{-3} mbar for 17 h and then leaving them under ambient dark conditions for 15 days.

Characterization of Samples. An atomic force microscopy (AFM) study was performed on photopolymerized samples using a JPK NanoWizard II system (JPK Instruments). The images were acquired in tapping mode, working in air in a vibration-insulated environment. Single-beam silicon cantilevers coated with aluminum on the reflective side (type AC160TS, Olympus) with typical elastic constant of 40 N m^{-1} and nominal tip radii of < 10 nm were used. The drive frequency was ~300 kHz, and the scan rate was between 0.2 and 1.0 Hz. Height was collected simultaneously with the amplitude and phase signals in both trace and retrace directions.

Adhesion force measurements were carried out in water with a JPK NanoWizard II AFM system. A cantilever with a triangular soft tip made of silicon nitride with a nominal elastic constant of 0.06 N m^{-1} was used, functionalized with thiol-terminated molecules (11-mercapto-1-undecanol). For each sample, we obtained the adhesion force values by analyzing 400 points on four different areas.

Fourier transform infrared (FT-IR) spectroscopy measurements in the 4000−1500 cm^{-1} spectral range were carried out using a VERTEX 70 FT-IR apparatus in absorbance mode at a resolution of 4 cm^{-1}.

Measurements of the apparent WCA, as defined by Marmur,[31] here called simply contact angle or WCA, were carried out with a KSV CAM200 instrument. Distilled water was used for these tests and was dispensed using a microsyringe. The typical drop volume was ~1 μL. For each sample, the contact angle value was obtained as an average of six measurements recorded on different adjacent areas of the surface.

To characterize the hysteresis of the samples, we measured the advancing and receding contact angles, θ_{adv}^h and θ_{rec}^h, respectively, by placing a water drop on the sample surface and tilting it until

(22) Wang, R.; Sakai, N.; Fujishima, A.; Watanabe, T.; Hashimoto, K. *J. Phys. Chem. B* **1999**, *103*, 2188–2194.

(23) Nakajima, A.; Koizumi, S.-I.; Watanabe, T.; Hashimoto, K. *J. Photochem. Photobiol., A* **2001**, *146*, 129–132.

(24) Sakai, N.; Wang, R.; Fujishima, A.; Watanabe, T.; Hashimoto, K. *Langmuir* **1998**, *14*, 5918–5920.

(25) Caputo, G.; Nobile, C.; Buonsanti, R.; Kipp, T.; Manna, L.; Cingolani, R.; Cozzoli, P. D.; Athanassiou, A. *J. Mater. Sci.* **2008**, *43*, 3474–3480.

(26) Caputo, G.; Nobile, C.; Kipp, T.; Blasi, L.; Grillo, V.; Carlino, E.; Manna, L.; Cingolani, R.; Cozzoli, P. D.; Athanassiou, A. *J. Phys. Chem. C* **2008**, *112*, 701–714.

(27) Caputo, G.; Cingolani, R.; Cozzoli, P. D.; Athanassiou, A. *Phys. Chem. Chem. Phys.* **2009**, *11*, 3692–3700.

(28) Sakai, N.; Fujishima, A.; Watanabe, T.; Hashimoto, K. *J. Phys. Chem. B* **2003**, *107*, 1028–1035.

(29) Sakai, N.; Fujishima, A.; Watanabe, T.; Hashimoto, K. *J. Phys. Chem.* **2001**, *105*, 3023–3026.

(30) Cozzoli, P. D.; Kornowski, A.; Weller, H. *J. Am. Chem. Soc.* **2003**, *125*, 14539–14548.

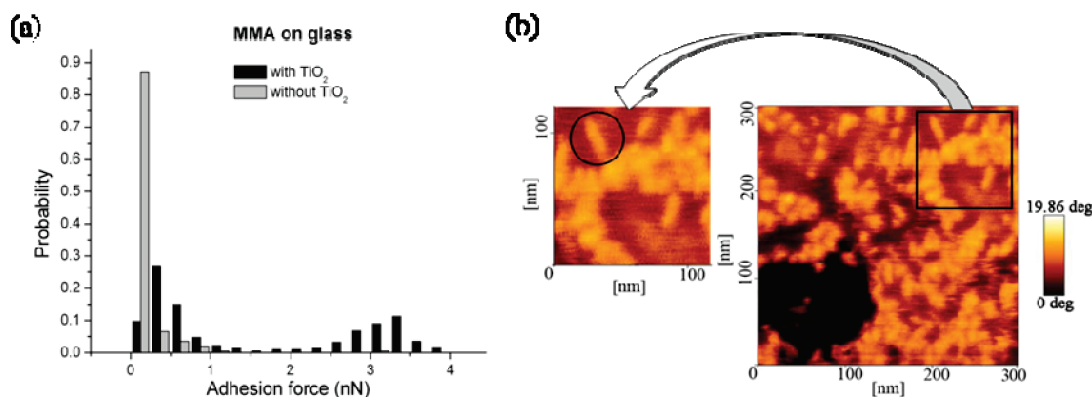(31) Marmur, A. *Soft Matter* **2006**, *2*, 12–17.

Figure 1. (a) Adhesion force peaks distribution in photopolymerized MMA on glass substrates with and without NRs. (b) AFM lateral force images of photopolymerized MMA/TiO₂ NRs (300 nm × 300 nm). In the inset is shown a magnified image where it is possible to distinguish single NRs (marked area).

the droplet began to slide. The angle subtended at the front of the drop is θ^h_{adv}, and that at the rear of the droplet is θ^h_{rec}. The magnitude of the hysteresis effect ($\Delta\theta^h$) was evaluated considering the difference between the advancing and the receding contact angles $\Delta\theta^h = \theta^h_{adv} - \theta^h_{rec}$. For this calculation, we considered the mean values of six different measurements performed on each surface, using a drop with a volume of 4 μL, to gain enough driving force from the gravity. Actually, the surface tilting process is a debated method because according to some authors,[32,33] the measured angles do not always correspond to the contact angles measured using the classical advancing and receding method. Nevertheless, the amount of data is too limited to draw any general conclusions and, according to recent studies,[34,35] this method is effective for the evaluation of the receding and advancing contact angles, mostly in the case of small drop volumes. Moreover, independent measurements done on our samples have shown that both advancing and receding contact angles have very similar values using the two methods. Details of these experiments can be seen in the Supporting Information (Figure S2).

Results and Discussion

Preparation, Characterization, and Wettability Measurements of the Nanocomposite Samples. Using the photopolymerization technique, we manage to produce nanocomposite patterned films of PMMA incorporating TiO₂ NRs on glass substrates, after 90 min of UV laser irradiation through aluminum photomasks. FT-IR spectra of the photopolymerized films confirm the completion of photopolymerization and the NR incorporation in the polymer matrix (Supporting Information, Figures S3 and S4).

The UV-induced reversible wettability changes of the TiO₂ NRs, used as nanofillers in the photopolymerized nanocomposites, can be exploited only if some NRs protrude out of the surface of the polymer matrix to be in contact with the liquid droplets. To obtain the NRs expulsion toward the surface of the produced films, MMA was the monomer of choice to be photopolymerized because of its poor chemical affinity with the

hydrophobic alkylic chains of the oleic-acid capping molecules of the NRs.[36−38] The incompatibility between the NRs capping molecules and the polymer matrix forces part of the NRs to move toward the surface of the nanocomposite films in the form of clusters (as will be demonstrated next) to minimize their interaction with the polar environment. Work is in progress on other nanocomposite systems using polymer matrices of higher chemical affinity with the NRs capping molecules to evaluate the differences in the NRs distribution in different matrices.

To verify the effective presence of the NRs exposed to the polymeric nanocomposite surface, we used a sensitive surface characterization method in which AFM tips are functionalized with hydrophilic molecules that interact with the surfaces by means of hydrophilic/hydrophobic forces. In particular, in Figure 1a, the distribution of the adhesion forces between the functionalized tips and the photopolymerized samples, with and without TiO₂ NRs, is presented. Because the capping molecules-free areas of the TiO₂ NRs are more hydrophilic compared with their organic environment (surfactants or polymer), they apply higher attraction forces to the hydrophilic functionalized tips. Indeed, the adhesion force values between the pure PMMA and the tips are always found to be < 1 nN, whereas in the case of the nanocomposite films, the values of the adhesion forces arrive up to 4 nN, with 44% of them > 1 nN, indicating the presence of organic-free inorganic TiO₂ regions, exposed on the top of the films. This finding is further supported by lateral force AFM images, as the one presented in Figure 1b, where the NRs are apparent on the surface of the photopolymerized MMA/TiO₂ nanocomposite film. In general, they appear quite aggregated on the surface of the samples; however, it is also occasionally possible to distinguish single NRs (inset of Figure 1b). In contrast, the photopolymerized coatings without TiO₂ NRs appear flat and homogeneous (Supporting Information, Figure S5).

We performed WCA measurements on the nanocomposite coatings to examine the effect of the presence of the TiO₂ NRs onto their surface on their wetting properties before and after UV excitation. Figure 2 illustrates the WCA values measured on prepared coatings with and without NRs, 48 h after their photopolymerization (1), after subsequent UV laser irradiation for 90 min (2), and after 17 h of vacuum storage (3), followed by 15 days in the dark (4).

The WCA of the pure photopolymerized MMA remains stable at 78 ± 2° throughout the irradiation and the recovery process, demonstrating that the TiO₂ NR-fillers are exclusively responsible for any wettability differences that may be induced by light. In the case of the photopolymerized MMA/TiO₂ nanocomposite films,

(32) Krasovitski, B.; Marmur, A. *Langmuir* **2005**, *21*, 3881–3885.
(33) Bormashenko, E.; Bormashenko, Y.; Whyman, G.; Pogreb, R.; Musin, A.; Jager, R.; Barkay, Z. *Langmuir* **2008**, *24*, 4020–4025.
(34) Lai, Y.-H.; Yang, J.-T.; Shieh, D.-B. *Lab Chip* **2010**, *10*, 499–504.
(35) Yang, J.-T.; Chen, J. C.; Huang, K.-J.; Yeh, A. *J. Microelectromech. Syst.* **2006**, *15*, 697–707.
(36) Zehner, R. W.; Lopes, W. A.; Morkved, T. L.; Jaeger, H.; Sita, L. R. *Langmuir* **1998**, *14*, 241.
(37) Shenhar, R.; Jeoung, E.; Srivastava, S.; Norsten, T. B.; Rotello, V. M. *Adv. Mater.* **2005**, *17*, 2206–2210.
(38) Pignatelli, F.; Carzino, R.; Salerno, M.; Scotto, M.; Canale, C.; Distaso, M.; Rizzi, F.; Caputo, G.; Cozzoli, P. D.; Cingolani, R.; Athanassiou, A. *Thin Solid Films* **2010**, *518*, 4425–4431.
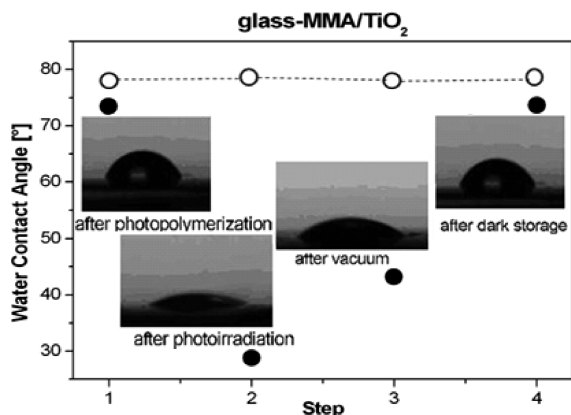
Figure 2. WCA measurements performed on nanocomposite photopolymerized MMA/TiO$_2$ NR films on glass during a cycle of UV irradiation and vacuum/dark storage (●) and of photopolymerized MMA films without NRs on glass during the same UV-irradiation/storage cycle (○). The thickness of the dots represents the experimental error of the measurements. The pictures of the water drops lying on the nanocomposite surface are shown at every step of the process.

the initial WCA is 73 ± 2°, lower than the one measured on the photopolymerized MMA films without NRs (78 ± 2°, step 1 in Figure 2). The decreased WCA value of the nanocomposite samples compared with that of the pure polymer may be attributed to diverse factors: to the increased hydrophilicity of TiO$_2$ NRs exposed on the surface of the films, as demonstrated by independent WCA measurements on films of TiO$_2$ NRs deposited by drop casting on glass substrates that gave an average WCA value of 72 ± 2°, or to the increased nanoroughness the NRs induce to the samples[35] (Supporting Information, Figure S5).

The UV irradiation of the nanocomposite films (step 2 in Figure 2) causes a dramatic decrease in $\Delta\theta = 45°$ in their WCA (WCA after UV excitation for 90 min becomes 28 ± 2°) due to the UV-induced hydrophilicity mechanism of TiO$_2$. Finally, after a short vacuum and dark storage period (steps 3 and 4 presented in Figure 2), the films totally recover their initial hydrophobic character. The reversible wetting cycles were repeated tens of times on various nanocomposite films without any apparent fatigue.

To elucidate the precise chemical mechanism responsible for the reversible wettability changes in the nanocomposite films upon UV irradiation and vacuum/dark storage, we performed FT-IR measurements. The relevant data are presented in Figure 3. The results reveal remarkable changes only in the OH band (3100–3650 cm^{-1}) of the nanocomposites. FT-IR measurements on pure PMMA polymer showed no changes before and after UV irradiation.

Specifically, upon UV irradiation, the signal from the hydroxyl groups of the molecularly physisorbed H$_2$O (ν(H$_2$O), ~3200 cm^{-1}) is substantially enhanced, suggesting an increase in hydroxylation on the exposed NRs facets. These OH species introduced to the surface upon photoirradiation are metastable because upon vacuum storage the related bands show a substantial reduction in intensity and, after subsequent dark storage, the initial surface hydroxylation degree is recovered. One widely accepted mechanism proposed in the literature for the TiO$_2$ wettability changes is in full agreement with our findings. In particular, upon UV excitation of TiO$_2$, holes are generated that react with lattice oxygen to form defects (oxygen vacancies).[25,26] At this point, ambient water molecules coordinate to these vacancies dissociatively or by physisorption; consequently, a very hydrophilic surface is created, as actually demonstrated by the decrease in the WCA measured in our experiment. Afterward, vacuum and dark storage permit the atmospheric oxygen to replace
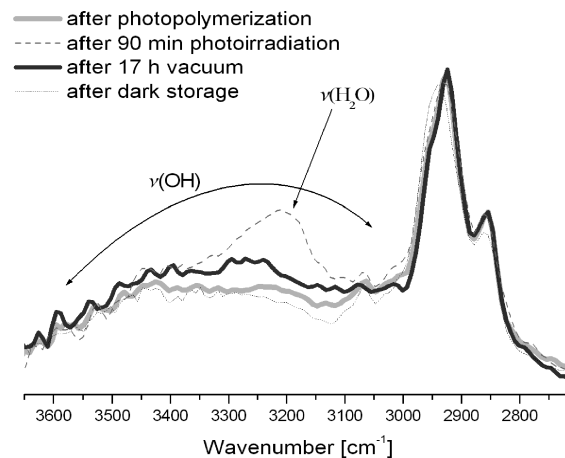

Figure 3. FT-IR spectra of photopolymerized MMA/TiO$_2$ films throughout a cycle of the UV irradiation and vacuum/dark storage process in the 3650–3100 cm^{-1} range.

the OH groups implanted onto the surface during the UV-driven hydrophilicization process, leading to the recovery of the initial hydrophobic state[25–27,39–44] and thus to the increase in the WCA.

Similarly to the WCA measurements, the FT-IR also shows that the nanocomposite films do not undergo any apparent fatigue after tens of irradiation/storage cycles because the representative polymer peaks remain unaffected by the irradiation process. Additionally, taking into account a previous study of our group,[25] which proved that using the above-mentioned irradiation conditions the organic capping molecules of the NRs do not undergo any photocatalytic destruction, we can safely assume that the photocatalytic property of TiO$_2$ does not play any important role in the specific experiment.

Drop Movement. Taking advantage of the increased wettability of the nanocomposite films upon UV irradiation, due to the presence of TiO$_2$ NRs, we can realize light-induced wettability gradients on the photopolymerized surfaces by irradiating adjacent surface areas for progressively longer time periods. This procedure allows us to create surfaces over which spontaneous water drop movement can be achieved. When a droplet is positioned at the boundary of two adjacent areas with different wettability, with the front edge experiencing the more hydrophilic area and the rear edge experiencing the less hydrophilic area, the driving force (F_d) that is acting on it is expressed by the following equation[45,46]

$$F_d = w\gamma \int_0^{\pi/2} (\cos\theta_f - \cos\theta_r)\cos\varphi\, d\varphi \qquad (1)$$

where w is the width of the drop, which equals twice the radius for a drop with a spherical-cap shape, γ is the surface tension of the water (72 mN m^{-1}), θ_f is the contact angle at the front edge, and θ_r is the contact angle at the rear edge of the drop (Figure 4).

(39) Zhang, Z.; Wang, C. C.; Zakaria, R.; Ying, J. Y. *J. Phys. Chem. B* **1998**, *102*, 10871.

(40) Wang, C.-Y.; Groenzin, H.; Shultz, M. J. *Langmuir* **2003**, *19*, 7330–7334.

(41) Finnie, K. S.; Cassidy, D. J.; Bartlett, J. R.; Woolfray, J. L. *Langmuir* **2001**, *17*, 816–820.

(42) Uosaki, K.; Yano, T.; Nihonyanagi, S. *J. Phys. Chem. B* **2004**, *108*, 19086–19088.

(43) Nosaka, A.; Fujiwara, T.; Yagi, H.; Akutsu, H.; Nosaka, Y. *J. Phys. Chem. B* **2004**, *108*, 9121–9125.

(44) Zhao, H.; Beysens, D. *Langmuir* **1995**, *11*, 627.

(45) Moumen, N.; Subramanian, R. S.; McLaughlin, J. B. *Langmuir* **2006**, *22*, 2682–2690.

(46) Subramanian, R. S.; Moumen, N.; McLaughlin, J. B. *Langmuir* **2005**, *21*, 11844–11849.
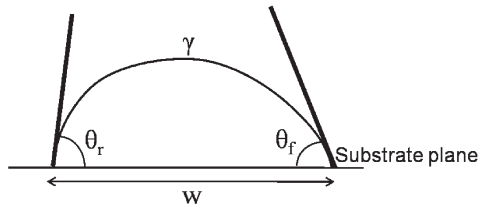
Figure 4. Sketch of the side view of a drop.

Because most surfaces are characterized by the phenomenon of contact angle hysteresis due to chemical or structural heterogeneities, demonstrated by the pinning of droplets onto them, for the motion to occur, this drop pinning should be overcome. Therefore, eq 1 is resolved using the hysteresis angles instead of the apparent angles to incorporate the hysteresis correction on the force acting on a drop with its front edge, *f*, lying on the area that has been irradiated for a longer time (so instead of *f*, we will use hereafter the notation "Mi" that stands for "more irradiated") and its rear edge, *r*, lying on the area that has been irradiated for a shorter time (so instead of *r*, from now on, we will use the notation "Li" that stands for "less irradiated"). Therefore, the hysteresis corrected net force F_d that acts on the drops can be expressed as

$$F_d = w\gamma(\cos\theta_{adv}^{hMi} - \cos\theta_{rec}^{hLi}) \quad (2)$$

where θ_{adv}^{hMi} is the advancing contact angle of the drop measured during the hysteresis experiment (tilted surface) on the area irradiated for a longer time and θ_{rec}^{hLi} is the receding contact angle of the drop measured during the hysteresis experiment on the area irradiated for a shorter time. The fundamental condition for the movement of the droplets to occur is that the driving force given by eq 2 is greater than the force opposing to this movement. The latter is the component of the so-called surface tension force (F_s) at the axis of the movement[47,48]

$$F_d \geq F_s \Rightarrow w\gamma(\cos\theta_{adv}^{hMi} - \cos\theta_{rec}^{hLi}) \geq w\gamma(\cos\theta_{rec}^{hLi} - \cos\theta_{adv}^{hMi}) \quad (3)$$

Resolving eq 3

$$\cos\theta_{adv}^{hMi} \geq \cos\theta_{rec}^{hLi} \Rightarrow$$
$$\theta_{rec}^{hLi} \geq \theta_{adv}^{hMi} \Rightarrow$$
$$\theta_{adv}^{hLi} - \theta_{rec}^{hLi} \leq \theta_{adv}^{hLi} - \theta_{adv}^{hMi} \Rightarrow$$
$$\Delta\theta^{hLi} \leq \Delta\theta_{adv}^h \quad (4)$$

Equation 4 represents the first criterion that is required for the drop movement to occur when the drop experiences at its edges two adjacent areas that have been irradiated for different times. This criterion is expressed as follows: The contact angle hysteresis of the rear area, irradiated for less time ($\Delta\theta^{hLi} = \theta_{adv}^{hLi} - \theta_{rec}^{hLi}$), must be smaller than the difference between the advancing contact angles of the two adjacent areas, measured with the tilted angle hysteresis experiment ($\Delta\theta_{adv}^h = \theta_{adv}^{hLi} - \theta_{adv}^{hMi}$).

The second criterion that needs to be fulfilled to achieve spontaneous, continuous, directional, and uninterrupted transport of the droplets throughout all adjacent surface areas that have been irradiated for progressively longer time periods, deals with the dimensions of the irradiated areas. More specifically, the water drop at its static state should have a diameter bigger than the side of each irradiated area at the direction of the movement lying underneath it so that it can experience constantly different contact angles at its two
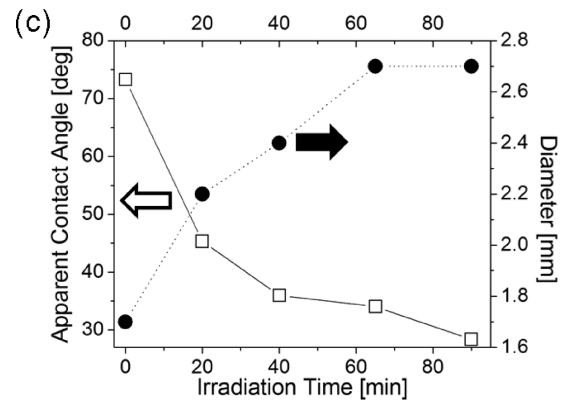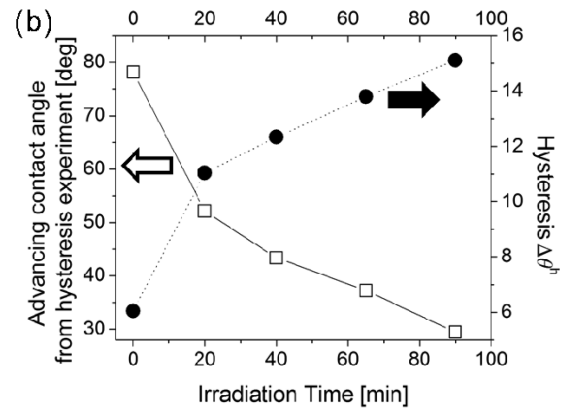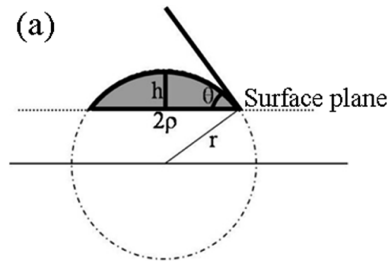
(47) ElSherbini, A. I.; Jacobi, A. M. *J. Colloid Interface Sci.* **2006**, *299*, 841–849.
(48) Gao, X.; Yao, X.; Jiang, L. *Langmuir* **2007**, *23*, 4886–4891.

Figure 5. (a) Sketch of a spherical cap and of the total sphere the cap belongs to (dotted line). (b) Advancing contact angles (—□—), measured using the tilted angle hysteresis experiment, and hysteresis values (···●···) on nanocomposite areas irradiated for different time. (c) Measured values of apparent contact angles (—□—) and calculated values of diameters (···●···) of droplets with a volume of 1 µL on nanocomposite areas irradiated for different time.

edges. The dimensions of each area can be appropriately designed depending on the volume of the water droplets and on the WCA of each area. In this work, we use drops with volume of 1 µL, which is small enough to assume that the shape of the drops is a spherical cap with height *h* and radius *ρ*, which belongs to a sphere of radius *r* (Figure 5a).[34]

The volume *V* of the droplets with a spherical-cap shape is given by eq 5

$$V = \frac{\pi h^2}{3}(3r - h) \quad (5)$$

with

$$r = \frac{h^2 + \rho^2}{2h} \quad (6)$$

Considering the apparent contact angle of the drop, θ, on a surface with homogeneous wettability, we can write

$$h^2 = \rho^2 (\tan \theta/2)^2 \qquad (7)$$

whereas eq 5 becomes

$$V = \frac{\pi}{6} \rho^3 \tan \frac{\theta}{2} \left(3 + \left(\tan \frac{\theta}{2} \right)^2 \right) \qquad (8)$$

Solving eq 8 for the radius of the drop, we find

$$\rho = \sqrt[3]{\frac{6V}{\pi \tan \frac{\theta}{2} \left(3 + \left(\tan \frac{\theta}{2} \right)^2 \right)}} \qquad (9)$$

Therefore, the second criterion for the drop movement to occur is that the side of each irradiated area along the direction of the movement should be smaller than the diameter of the drop on the specific area, given by twice the drop radius ρ (calculated using eq 9).

The validity of the first criterion can be easily assessed for adjacent areas irradiated with increasing time using Figure 5b. In this Figure are presented the values of the advancing contact angles, measured using the tilted angle hysteresis experiment and the hysteresis values on different nanocomposite areas as a function of their irradiation time. For the proper design of surface areas satisfying the second criterion, Figure 5c can be used. In this Figure, the diameters of 1 μL volume droplets (calculated using eq 9), together with the measured apparent contact angle values θ on the respective nanocomposite areas, as a function of their irradiation time, are presented.

Following both criteria above as requirements for the drop movement to occur, we created a surface wettability gradient by irradiating adjacent areas for 0, 40, and 90 min. The diameters of 1 μL drops situated on the differently irradiated areas have been calculated using eq 9. Specifically, the drops placed on the nonirradiated area with WCA 73 $\pm$ 2° have 1.79 mm diameter, those placed on the 40 min irradiated area with WCA 36 $\pm$ 2° have a diameter of 2.40 mm, and those positioned on the 90 min irradiated area with WCA 28 $\pm$ 2° have 2.72 mm diameter. Therefore, to fulfill the second criterion, which describes that the drops should experience constantly different contact angles at their two edges, we realized an X$\times$Y = 5 $\times$ 5 mm^2 photopolymerized pattern of nanocomposite film using a proper aluminum mask. To achieve the movement along the X axis, a first area of X$\times$Y = 1 $\times$ 5 mm^2 was left without irradiation and two adjacent areas of X$\times$Y = 2 $\times$ 5 mm^2 each, were irradiated for 40 and 90 min, respectively. In this way, the diameter of the drop on each area always remains bigger than the side of the area along the direction of the drop movement. On the first nonirradiated area, the contact angles measured with the tilted angle hysteresis experiment were $\theta_{adv}^h = 78 \pm 2$° and $\theta_{rec}^h = 72 \pm 2$° ($\Delta\theta^{h'} = 6$°), whereas on the 40 min irradiated area, $\theta_{adv}^h = 43 \pm 2$° and $\theta_{rec}^h = 31 \pm 2$° ($\Delta\theta^{h''} = 12$°). The smaller hysteresis value of the nonirradiated area compared with the irradiated one is in agreement with various observations in the literature mentioning that the hysteresis increases as the hydrophilicity of the surfaces increases.[33,34,43−45] Meeting the requirements of the first criterion, the difference of the advancing contact angles between the first and the second area measured at the hysteresis experiments ($\Delta\theta_{adv}^h = 78 - 43 = 35$°) is greater than the contact angle hysteresis at the first area, $\Delta\theta^{h'}$. Analogously, the advancing contact angle measured
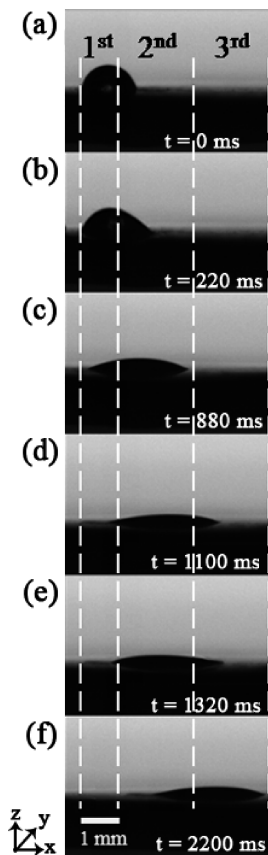

Figure 6. Side view photographs of a water droplet that is moving on a PMMA/TiO$_2$ surface with UV-induced gradient hydrophilicity. The hydrophilicity increase is in the direction of the drop movement, from left to right. In each frame is indicated the time t passed after the drop deposition ($t = 0$ ms).

in the hysteresis experiment on the 90 min irradiated area was $\theta_{adv}^h = 29 \pm 2$°; therefore, the difference of the advancing contact angles between the second and the third areas ($\Delta\theta_{adv}^h = 43 - 29 = 14$°) is greater than the contact angle hysteresis at the second area, $\Delta\theta^{h''}$. Figure 6 shows the transport of a 1 μL water droplet on the 5 $\times$ 5 mm^2 nanocomposite film, designed as described above.

By analyzing the frames taken during the drop motion presented in Figure 6, it can be seen that initially the droplet was placed at the interface between the first nonirradiated area and the second region so that its front part is in contact with the second area irradiated for 40 min (Figure 6a). Immediately after placing the drop, its front edge starts to move, causing the elongation of the drop toward the area with higher hydrophilicity, whereas the rear edge initially does not move because of the pinning or hysteresis effect of the NR-rich surface (Figure 6b,c).[10,49] As the droplet fills completely the second area, and its front edge experiences the third even more hydrophilic area, its rear edge also moves forward (Figure 6d,e). Finally, when the drop fills the third area entirely, its movement stops (Figure 6f). A movie in AVI format demonstrating the real time movement of the drop is available in the HTML version of this Article. As reported in several studies,[8,9,45] this kind of motion is due to a large spatial gradient in the surface tension across the droplet, caused by the wettability change along the nanocomposite surface. This so-called capillary force overcomes droplet pinning and leads to the drop transport.

(49) Marmur, A. *Langmuir* **2008**, *24*, 7573−7579.

Conclusions

We demonstrate the realization of nanocomposite materials with tailored surface properties and reversible surface wettability using photopolymerization of solutions of monomers (MMA) and TiO$_2$ NRs. The response of the latter to UV light generates the switchable wettability on the nanocomposite surfaces. Taking advantage of this property, we present a strategy for the realization of paths with increasing hydrophilicity gradient, on which spontaneous motion of water droplets is induced. Liquid droplet motion in the direction of the hydrophilic gradient is achieved by irradiation of adjacent surface areas with increasing time. These results provide additional understanding of the control of drop motion with the use of light.

The combination of the photopatterning with the use of the time-dependent hydrophilicity changes of the TiO$_2$-filled nanocomposites opens up a large number of possibilities for the use of these systems in advanced fluidic systems. The reversibility of the light-induced hydrophilicity, obtained by coupling the vacuum treatment to the dark ambient storage, makes these systems very attractive because they can be reprocessed and reused.

Supporting Information Available: TEM image of the MMA/TiO$_2$NRs/PI solution, images of water drops for the measurement of the advancing and receding contact angles with both the classical and the tilting surface methods, FT-IR spectra of photopolymerized MMA/TiO$_2$NRs sample and for as-received PMMA with TiO$_2$ NRs, and AFM images of photopolymerized MMA samples with and without NRs. This material is available free of charge via the Internet at http://pubs.acs.org.